ACS APPLIED MATERIALS & INTERFACES

www.acsami.org

Research Article

# Insights into Superlow Friction and Instability of Hydrogenated Amorphous Carbon/Fluid Nanocomposite Interface

Xiaowei Li,* Xiaowei Xu, Jianwei Qi, Dekun Zhang, Aiying Wang,* and Kwang-Ryeol Lee*

Cite This: *ACS Appl. Mater. Interfaces* 2021, 13, 35173−35186

Read Online

ACCESS | Metrics & More | Article Recommendations | Supporting Information

**ABSTRACT:** Hydrogenated amorphous carbon (a-C:H) film exhibits the superlubricity phenomena as rubbed against dry sliding contacts. However, its antifriction stability strongly depends on the working environment. By composting with the fluid lubricant, the friction response and fundamental mechanisms governing the low-friction performance and instability of a-C:H remain unclear, while they are not accessible by experiment due to the complicated interfacial structure and the lack of advanced characterization technique in situ. Here, we addressed this puzzle with respect to the physicochemical interactions of a-C:H/oil/graphene nanocomposite interface at atomic scale. Results reveal that although the friction capacity and stability of system are highly sensitive to the hydrogenated degrees of mated a-C:H surfaces, the optimized H contents of mated a-C:H surfaces are suggested in order to reach the superlow friction or even superlubricity. Interfacial structure analysis indicates that the fundamental friction mechanism attributes to the hydrogenation-induced passivation of friction interface and squeezing effect to fluid lubricant. Most importantly, the opposite diffusion of fluid oil molecules to the sliding direction is observed, resulting in the transformation of the real friction interface from a-C:H/oil interface to oil/oil interface. These outcomes enable an effective manipulation of the superlow friction of carbon-based films and the development of customized solid−fluid lubrication systems for applications.

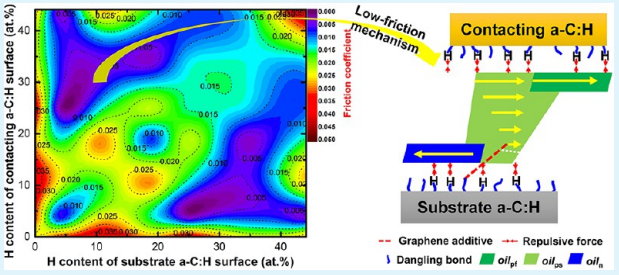


**KEYWORDS:** *hydrogenation, fluid lubricant, amorphous carbon, friction mechanism, reactive molecular dynamics*



## 1. INTRODUCTION

Due to the superlubricity phenomena (i.e., $\mu$ ~0.001) under dry and high vacuum conditions, hydrogenated amorphous carbon (a-C:H) film as a fantastic solid lubricant arouses many scientific and engineering interests in the high-tech fields, such as automobile, advanced manufacturing, artificial joint, robotics, aerospace, et al.[1−4] This attributes to the pivotal impact of hydrogen in films, reducing the shearing strength of mated surfaces through H-induced interfacial passivation and repulsive forces, as proposed by both the experimental[5,6] and theoretical results.[7−9] But a-C:H film also shows high sensitivity to the environment ($O_2$, $H_2O$, et al.),[10−12] disabling its antifriction capacity by the surface dehydrogenation or the formation of the low-density surface shear band.[13]

Recently, in order to satisfy the ever-growing requirements for the superlubricity performance at the macroscale and the long-term reliability of key moving components, the synergistic combination of amorphous carbon nanostructure and fluid lubricant becomes a matter of great concern.[2,14−19] For the a-C film as solid lubricant, including H-free and H-containing cases,[1,20] it has excellent self-lubrication property and thus can improve the tribological property of coated surface significantly.[16,21,22] Most importantly, it can effectively overcome the risk of friction-wear failure under instantaneous oil-free or oil-starved conditions, such as the start/stop period of engine.[23] For the fluid lubricant, it is normally composed of base oil and lubricant additives, in which the base oil could not only enhance the antifriction behavior by hydrodynamic lubrication and weaken the environmental sensitivity of a-C, but also separate the mated a-C surfaces against their cold welding[14,15] and self-consumption. While the lubricant additive, especially that with graphene-like structure, can modify the tribological performance via the formation of a protective film with low shearing strength at the sliding contact zone,[18,19,24,25] it can also enhance the load-bearing capacity of base oil against dissociation.[26,27]

It is well-known that the antifriction capacity of a-C:H/oil/additive nanocomposite system is closely related with the surface/interface structure. The hydrogenated degree of a-C:H film can be tailored in a large scale (0~50% for H content).[1] The combination of a-C:H films with different surface hydrogenated states brings the different interfacial structures, potentially affecting the physicochemical properties of fluid lubricant at the sliding interface, such as adsorption, wetting, etc. Previous

Received: May 21, 2021
Accepted: July 7, 2021
Published: July 19, 2021

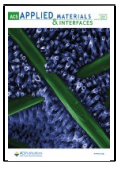




https://doi.org/10.1021/acsami.1c09432
*ACS Appl. Mater. Interfaces* 2021, 13, 35173−35186

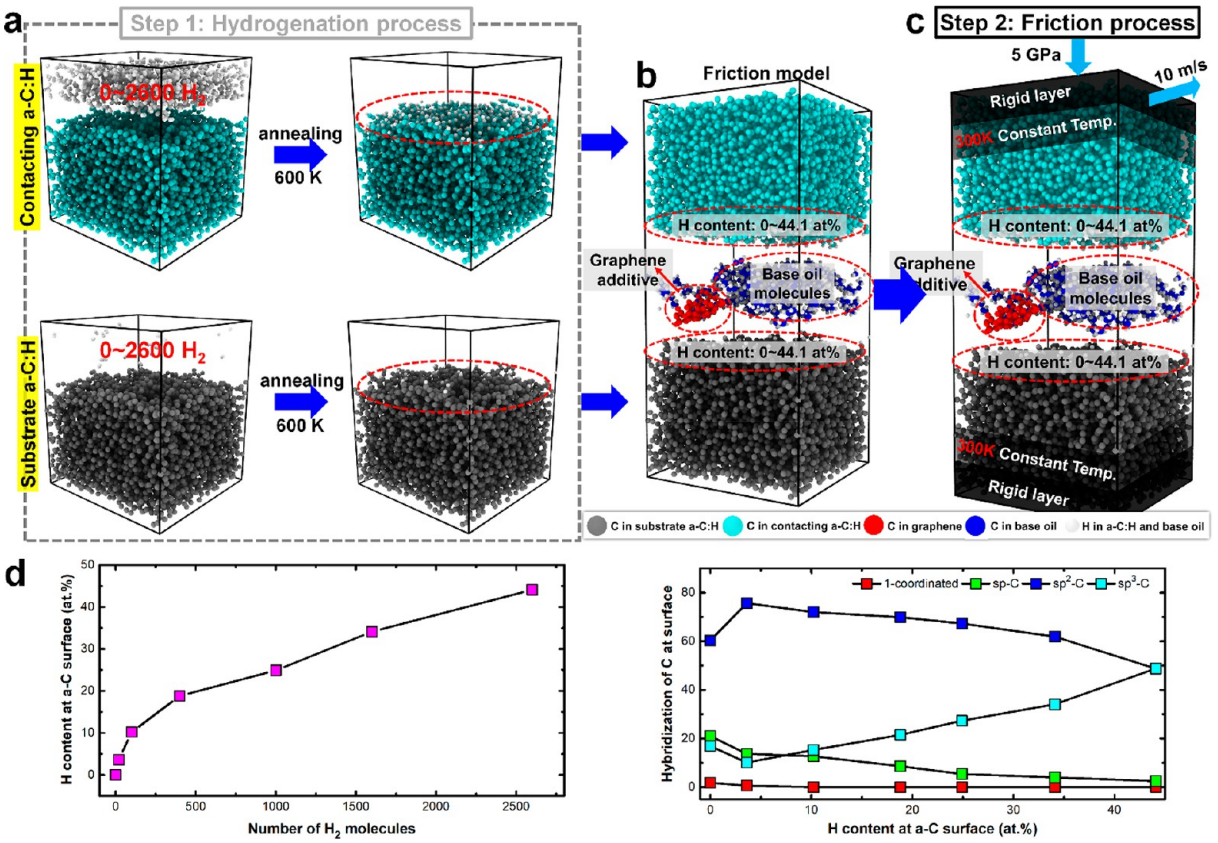


**Figure 1.** "*Two-step*" simulation process and structural analysis of fabricated a-C:H. (a) hydrogenation process of intrinsic a-C surface at 600 K; (b) friction model; (c) friction process under the fixed contact pressure of 5 GPa and sliding velocity of 10 m/s; (d) structural transformation of fabricated a-C:H film.

experiments and simulations have fully clarified that under the dry condition, the friction coefficient as a function of the surface H contents of mated a-C surfaces monotonically decreased.[5−9] However, under the lubricant condition, the effect of the hydrogenated degree of a-C:H surface on the physicochemical behaviors of base oil and additive is still not fully understood yet. Which combinatorial model of mated a-C:H surfaces is the most favorable to reduce the friction remains vague, while it cannot be achieved in the experiment without numerous heuristic experiments. Moreover, due to the lack of advanced characterization technique in situ, even less is known about the details of the most essential information on the thin friction interface, such as the interactions of additive and base oil with a-C:H and their transformation with increasing the hydrogenated degree of a-C:H surface. To the best of our knowledge, there are no experimental or simulation reports yet about this information, which are the key clues to disclose the underlying antifriction mechanism and provide the roadmap for technical and engineering applications.

In light of these considerations and also based on our previous studies,[19,24] we selected graphene as an additive and linear alpha olefin (AO), $C_8H_{16}$, as a representative base oil, respectively, to composite with the a-C:H films. Using reactive molecular dynamics (RMD) simulation, the tribo-induced interface of a-C:H/oil/graphene synergy system was mainly investigated for the purpose of understanding how hydrogenated degrees of mated a-C:H surfaces affect the frictional properties and their interaction with graphene additive and AO oil. First, we designed the a-C:H films with different surface H contents by hydrogenating the intrinsic a-C structure at 600 K (Figure 1a). Then, we built the a-C:H/oil/graphene model (Figure 1b) to simulate the friction process, in which the combinatorial screening of different a-C:H films as mating materials was considered (Figure 1c). Last, we suggested the optimized model of mated a-C:H films to achieve excellent antifriction performance and clarified the underlying mechanism. These outcomes advance the frontiers of scientific knowledge, which not only shed light on the origin of friction instability of a-C:H films as combined with fluid lubricant, but also guide the development and practical application of high-efficient a-C:H lubrication system.

## 2. METHODS

**Fabrication of a-C:H Film.** Large-scale Atomic/Molecular Massively Parallel Simulator code[28] was adopted to perform all RMD calculations. In order to evaluate the effect of surface hydrogenated degree on the friction stability of a-C:H/oil/graphene system, the a-C:H models with different surface H contents were fabricated. First, the intrinsic a-C structure was deposited via atom-by-atom deposition approach,[29] which has a size of 42.88 × 40.36 × 31.00 Å$^3$ and was composed of 6877 C atoms. Then, to carry out the hydrogenation process (Figure 1a), high-pressure $H_2$ gas was introduced into the top vacuum space of a-C substrate following the annealing treatment of system at 600 K for 125 ps with Nose-Hoover thermostat.[30] The number of $H_2$ molecules in the model was increased from 20 to 2600 in order to tailor the H content of a-C:H surface. Previous study[9] has also confirmed that 600 K was appropriate to change the structure of a-C surface only without deteriorating the intrinsic structure. After that, the system was cooled to 300 K and the detailed simulation process was given in our previous study.[9]

**Friction Model of a-C:H/Oil/Graphene Nanocomposite System.** The "*sandwich*" friction model was built for each case, as


https://doi.org/10.1021/acsami.1c09432
ACS Appl. Mater. Interfaces 2021, 13, 35173−35186

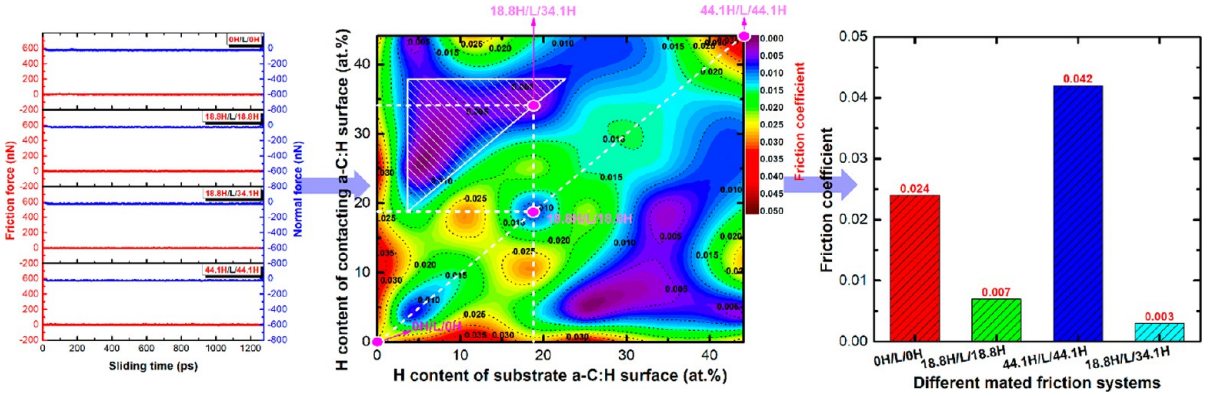


**Figure 2.** Friction results of a-C:H/oil/graphene nanocomposite system, including the friction curves with sliding time and friction coefficient.

shown in Figure 1b, including substrate a-C:H, contacting a-C:H, and fluid lubricant. For the substrate and contacting a-C:H films, the surface H content ranged from 0 to 44.1 at. %, respectively. The fluid lubricant consisted of $C_8H_{16}$ base oil with 45 molecules[31] and graphene as additive. The graphene structure was composed of 60 C atoms and its efficiency of reducing the friction coefficient has been confirmed in previous studies by comparing with other carbon nanoparticles (fullerene, carbon nanotube, etc.).[18,24] In the following study, the friction model was abbreviated as $c_1$H/L/$c_2$H, where $c_1$ and $c_2$ corresponded to the surface H contents (unit: at.%) of substrate and contacting a-C:H films, respectively; L represented the fluid lubricant including $C_8H_{16}$ oil and graphene additive. The initial surface of fluid lubricant was 3 Å away from the substrate and contacting a-C:H films.

**Friction Process and Parameters.** Before the friction process, Figure 1c showed that the whole system was divided into three layers, including rigid layer, thermostatic layer at 300 K using microcanonical ensemble with Berendsen thermostat,[32] and free layer; the details could be found in our previous work.[9,24] During the friction process, the system was first relaxed at 300 K for 2.5 ps, and then a normal force was applied to the top rigid layer of contacting a-C:H film to achieve a constant contact pressure of 5 GPa during 25 ps. After that, this top rigid layer moved along the $x$ direction with a constant velocity of 10 m/s in order to adequately sample the phase structure during the short MD simulation time;[14,33] the total sliding time was 1.25 ns. After the friction process, the friction coefficient ($\mu$) was calculated using the following equation:

$$\mu = \frac{f}{W} \tag{1}$$

where the frictional force, $f$, was calculated by summing the force acting on the rigid layer of substrate a-C:H model along the sliding direction; $W$ was the normal force. In addition, the cases without graphene additive were also considered for comparison. The time step of 0.25 fs was used and periodic boundary condition was applied along the $x$- and $y$ directions. Reactive force field potential developed by Tavazza[34] was used to describe the interactions between base oil, graphene, and a-C:H films.

## 3. RESULTS AND DISCUSSION

**Microstructure of a-C:H Film after Surface Hydrogenation.** In order to fabricate the a-C:H films with different hydrogenated degrees, the intrinsic a-C is annealed at 600 K under different $H_2$ environments, as shown in Figure 1a. After the hydrogenation process, it is found that the evolution of a-C structure mainly occurs at the surface above 27 Å without deteriorating the intrinsic a-C structure (Figure S1 of Supporting Information (SI)). The further structure analysis of a-C:H film in Figure 1d shows that as the number of $H_2$ molecules increases from 0 to 2600, the H content at a-C:H surface (region with gray background in SI Figure S1) ranges from 0 to 44.1 at. %. In particular, the sp-C fraction with H content of a-C:H surface significantly decreases from 21.0 at. % to 2.5 at. % (Figure 1d). However, when the surface H content increases from 0 to 3.6 at. %, the change of $sp^2$-C fraction increases following the drop of $sp^3$-C fraction, which is due to the thermal-induced $sp^3$-to-$sp^2$ transformation.[35,36] With further increasing the H content to 44.1 at. %, the large amount of H atoms bond with both the sp-C and $sp^2$-C atoms to form the $sp^3$-C hybridized structure, accounting for the change of hybridized structure at a-C surface. In addition, our previous study[9] has confirmed that after the hydrogenation process the obtained a-C:H films possessed similar roughness values.

**Friction Dependence on Mated a-C:H Surface Structures.** Under the lubricant condition, the dependence of antifriction behaviors on H contents of mated a-C:H surfaces are demonstrated in Figure 2. First, the evolutions of friction force and normal force curves with sliding time reveal that for each case, the system can reach the stable friction stage with almost no running-in process. The friction coefficient for each system is calculated using the values of friction force and normal force during the last sliding time of 200 ps, as given in Figure 2. Note that compared to the H-free case, hydrogenating the a-C surface could improve the friction behavior of a-C:H/oil/graphene nanocomposite system, but the friction coefficient as a function of H contents of mated a-C:H surfaces is flexible while has no monotonously decrease as observed under dry condition.[9]

For the self-mated a-C:H films, when the surface H content increases from 0 to 18.8 at. %, the friction coefficient decreases from 0.024 to 0.007, while it increases to 0.042 as the surface H content reaches 44.1 at. %. Especially, when the a-C:H films with different hydrogenated degrees are contacted, the superlow friction coefficient tends to be obtained. For example, in the 18.8H/L/34.1H, the friction coefficient is only 0.003. So according to the mapping of friction coefficient with H contents of mated a-C:H surfaces, a region is approximately suggested for a-C:H/oil/graphene lubrication system (marked with shadow in Figure 2), in which the ultralow friction ($\mu$ < 0.003) can be normally obtained. In this region, the relationship of the H contents of mated a-C:H surfaces is described as following:

$$38 \geq y \geq x + 15.2 \text{ in which } 3.6\text{at. \%} < x < 22.8\text{at. \%} \tag{2}$$

where $x$ and $y$ are the surface H contents of substrate and contacting a-C:H films, respectively.

**Interaction between a-C, $C_8H_{16}$ Oil, And Graphene Additive.** The friction behavior is strongly dependent on the interfacial structure and the hydrodynamic behavior of fluid


https://doi.org/10.1021/acsami.1c09432
ACS Appl. Mater. Interfaces 2021, 13, 35173−35186

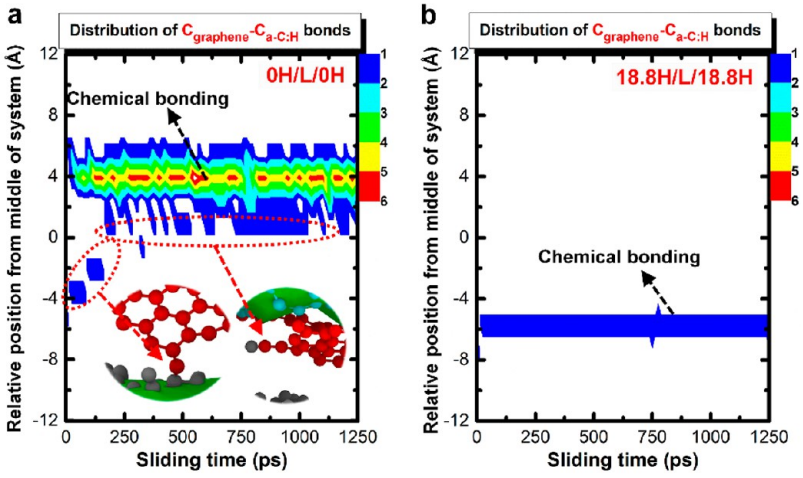


**Figure 3.** Distribution of $C_{graphene}$-$C_{a\text{-}C:H}$ bond number during the sliding process for the systems of (a) 0H/L/0H and (b) 18.8H/L/18.8H, respectively.

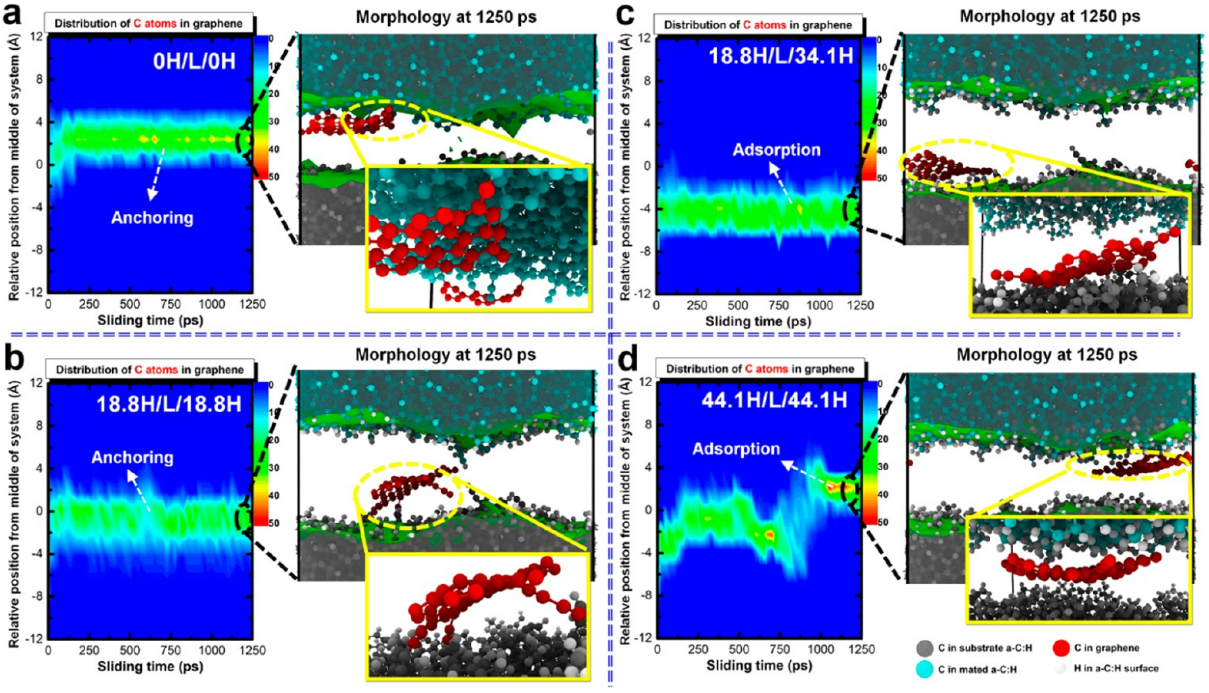


**Figure 4.** Distribution of C atoms in graphene and corresponding morphologies of friction interfaces (the base oil molecules are neglected for view) after sliding process for the systems of (a) 0H/L/0H, (b) 18.8H/L/18.8H, (c) 18.8H/L/34.1H, and (d) 44.1H/L/44.1H, respectively.

lubricant.[14−16,24] In order to clarify the underlying friction mechanism caused by different mated a-C:H films, the interactions between a-C:H film, graphene additive, and $C_8H_{16}$ base oil are explored. First, the introduction of fluid lubricant could effectively prevent the mated a-C:H films from cold welding, as shown in SI Figure S2. Moreover, due to the relatively low contact pressure applied in this work, $C_8H_{16}$ base oil has no chemical bonding with graphene additive or mated a-C:H films, which is similar to previous works.[15,19,24] In addition, H atoms at mated a-C:H surfaces interact with base oil and graphene additive in the form of intermolecular interaction; they stably exist at the a-C:H surfaces without the breaking of C−H bond (SI Figure S2) and the formation of hydrogen molecular during the friction process. This is different from the reports by A. Erdemir[16] and M. Kubo.[37]

However, the interaction of graphene additive with a-C:H film exhibits strong sensitivity to the hydrogenated degrees of mated surfaces. Taking the 0H/L/0H, 18.8H/L/18.8H, 18.8H/L/34.1H, and 44.1H/L/44.1H systems for examples, Figure 3 and Figure 4 give the distribution of bond number between graphene and C atoms in a-C:H ($C_{graphene}$-$C_{a\text{-}C:H}$), distribution of C atoms in graphene, and interfacial snapshots after sliding time of 1250 ps. The mean-square displacement curve (MSD) of graphene additive[24] is also plotted in Figure 5a for each case. For the H-free system (Figure 3a), the graphene additive first bonds with the substrate a-C surface, causing one C atom detached from the substrate, and then quickly interacts with the dangling bond of contacting a-C surface by strong chemical bonding during the sliding process (SI Movie S1). This anchoring state makes graphene additive stabilized to one a-C surface as a protective film (Figure 4a), smoothing the a-C surface, as reported by


https://doi.org/10.1021/acsami.1c09432
ACS Appl. Mater. Interfaces 2021, 13, 35173−35186

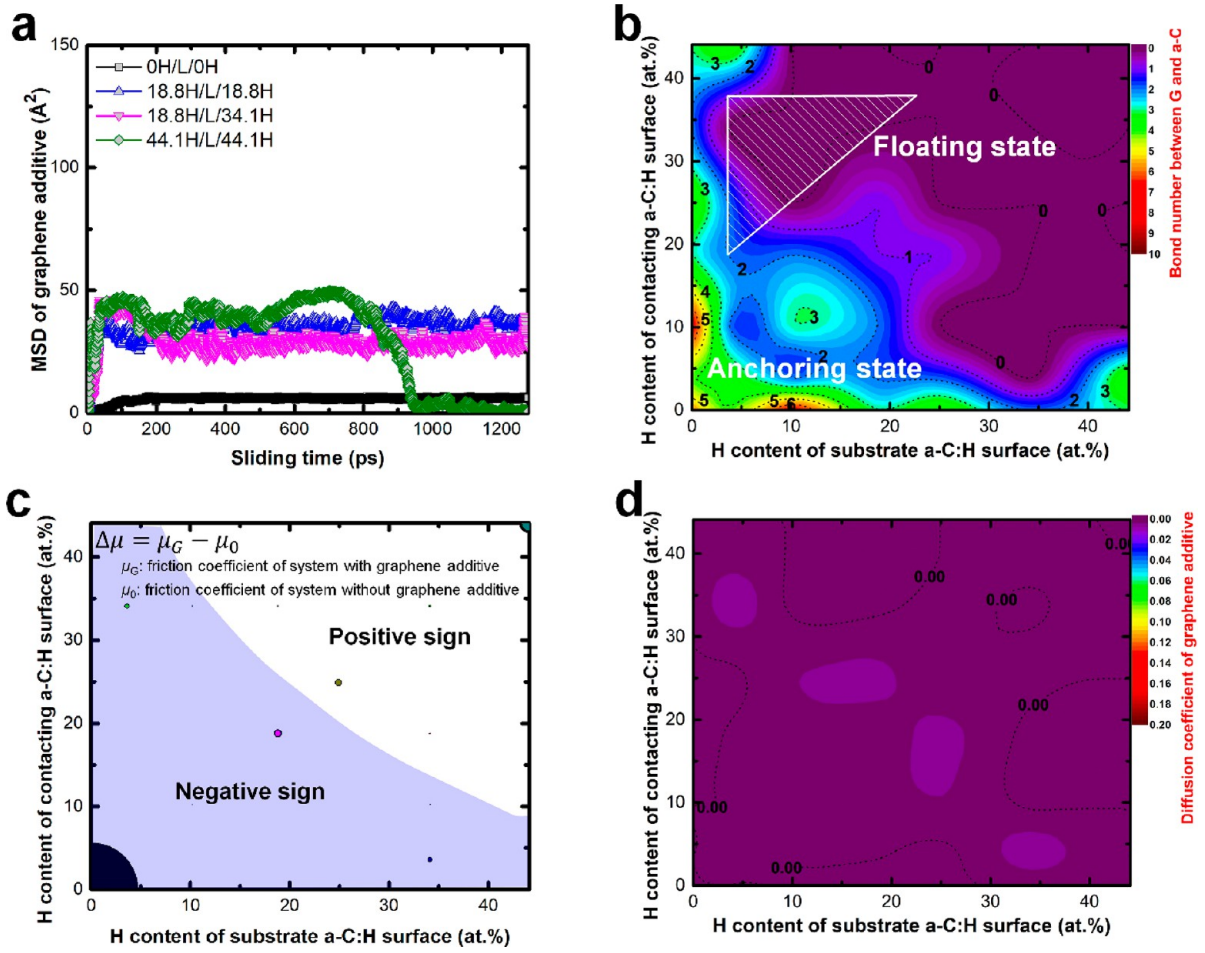


**Figure 5.** Behavior of graphene additive at friction interface. (a) MSD curves of graphene additive for 0H/L/0H, 18.8H/L/18.8H, 18.8H/L/34.1H, and 44.1H/L/44.1H systems. (b) Change of bond number between G and a-C:H with H contents of mated a-C:H surfaces. (c) Difference of friction coefficient between systems with/without graphene additive and its change with H contents of mated a-C surfaces, in which the ball size corresponds to the value difference. (d) Diffusion coefficient of graphene additive as a function of H contents of mated a-C:H surfaces.

previous studies.[19,38,39] This can be also confirmed by the small MSD values in Figure 5a. Similar behavior is also observed for the 18.8H/L/18.8H system, as shown in Figure 3b and Figure 4b. However, although the graphene additive in this system can also anchor to a-C:H surface, it shows the weakened bonding strength between graphene additive and a-C:H (Figure 3b). This is due to the increased H content of a-C:H surface, passivating the dangling bonds and thus weakening the intermolecular interaction of a-C:H to graphene. Combined with the repulsive force of H atoms from a-C:H,[7,9] the unbonded part of graphene structure exhibits a relatively large fluctuation (Figure 4b, SI Movie S2). This can be confirmed by the slightly high MSD value in Figure 5a, but it will also affect the distribution of base oil molecules during the sliding process.

For the 18.8H/L/34.1H system (Figure 4c), with the further improvement of hydrogenated degrees of mated a-C:H surfaces, there is no any covalent bond observed between graphene additive and a-C:H, suggesting the floating state of graphene. This inevitably induces the increased mobility of graphene structure at the initial sliding state when compared to the anchored cases (Figure 5c), but similar to the 18.8H/L/18.8H system. In addition, for this nonself-mated system, the graphene additive tends to be deviated to the a-C:H surface with a relatively low passivated degree during the sliding process (SI Movies S3). In particular, for the highly hydrogenated 44.1H/L/44.1H system (Figure 4d and Figure 5a), after the running-in period of graphene with mated a-C:H films and base oil, the graphene additive shows the physically stable existence at this a-C:H/oil interface in the form of floating state (SI Movies S4). In addition, the graphene structure is parallel to the sliding direction (Figure 4d). This phenomenon is not only due to the intermolecular interaction from a-C:H but also mainly caused by the squeezing effect of H repulsive stress from contacted base oil and a-C:H film, as will be discussed later.

In order to further quantify the effect of mated a-C:H surface structures on graphene additive, the bond number between graphene additive and a-C:H after the sliding process is counted and its dependence on the H contents of mated a-C:H surfaces is given in Figure 5b. It clearly illustrates that increasing the surface H content reduces the active sites of a-C:H surface and thus results in the transformation of binding state between graphene and a-C:H from chemical anchoring to physical floating state. Especially for these systems with anchored graphene, the increase of H content in mated a-C:H surfaces weakens the chemical strength between graphene additive and a-C:H film (Figure 5b). However, due to the absence of cross-linking between mated a-C:H films and graphene,[24] there is no obvious dissociation of graphene structure observed.

**Role of Graphene Additive at the Mated a-C:H Surface.** Through the comparison among the results in Figure 2 and


https://doi.org/10.1021/acsami.1c09432
ACS Appl. Mater. Interfaces 2021, 13, 35173−35186

Figure 5b, the system with strongly anchored or fully float graphene normally exhibits a relatively high friction coefficient, while the superlow friction phenomena normally occur in the transition region of graphene binding state from weak covalent bonding to floating state. In such transition, mated a-C:H surfaces have medium H contents, such as 18.8H/L/18.8H and 18.8H/L/34.1H. On the one hand, the graphene with no and weak bonding at a-C:H surface could strongly disturb the distribution and mobility of base oil molecules by its side atoms with high activity, as confirmed by SI Movies S2 and S3, and thus affect the friction behavior. This is different from the smoothing effect of graphene strongly anchored onto the poorly hydrogenated a-C:H surface (Figure 4a) and will be further discussed by the following analysis of base oil. On the other hand, this suggests that the role of graphene additive strongly depends on the H contents of mated a-C:H surfaces. The graphene additive can reach the maximally synergistic effect with the moderately hydrogenated a-C:H in reducing the friction. While for these systems with excess surface H content, the physical adsorption of graphene additive (Figure 4d) at the a-C:H/oil interface will weaken or shield the strong repulsive interaction between H atoms from a-C:H and base oil,[24] resulting in the extra increase of shearing resistance.

In order to further confirm this point, the friction simulations of systems without graphene additive are conducted. The difference of friction coefficient between systems with/without graphene additive, $\Delta\mu$, is calculated as follows.

$$\Delta\mu = \mu_G - \mu_0 \quad (3)$$

where $\mu_G$ and $\mu_0$ are the friction coefficients of systems with and without graphene additive, respectively. Figure 5c displays the change of $\Delta\mu$ with H contents of mated a-C:H surfaces, which changes from negative to positive sign. This indicates the role of graphene additive in friction reduction evolved from positive to negative effect. For the mated a-C surface with H-free or moderate H-passivation, the graphene can anchor or adsorb on the bare site of a-C surface with more dangling bonds. So it plays a positive role in reducing the friction coefficient which is also contributed by the H-induced passivation and repulsive effect.[5−9]

On the contrary, for the highly H-passivated a-C surface (such as 44.1H/L/44.1H), as compared to the case without additive, the introduction of graphene additive brings the unexpected increase of friction coefficient (Figure 5c), indicating the negative role of graphene additive in friction reduction. This physical adsorption of graphene on highly hydrogenated a-C:H surface decreases the repulsive force of H from a-C:H surface without obvious change of those from $C_8H_{16}$ bae oil (SI Figure S3). This G-induced suppression on the strong a-C:H/oil repulsive interaction will lower the driving force for the diffusion of oil molecules. Moreover, for each system, whatever the chemical anchoring or physical floating state of graphene, the calculated diffusion coefficient of graphene structure is shown in Figure 5d. It is close to zero for each case, much smaller than that of base oil. So in the present work, the mobility of graphene additive should play a limited role on the change of friction behavior with hydrogenated degree of a-C:H surface. But its contribution, originating from the effect of different binding states (Figure 4 and Figure 5b) on the distribution and mobility of base oil and the a-C:H/oil interaction, should be considered.

**Structural Evolution of Friction Interface Induced by Hydrogenation.** Figure 6 shows the changes of interfacial hybridized structure with sliding time for the 0H/L/0H, 18.8H/L/18.8H, 18.8H/L/34.1H, and 44.1H/L/44.1H systems, respectively, which is only contributed by the C atoms from a-C:H and graphene additive. Note that the evolution of hybridized structure with sliding time depends on the hydrogenated state of a-C:H surface. For the friction systems with bare or poorly hydrogenated a-C:H surfaces, such as 0H/L/0H, there is a high fraction of sp-C dangling bond (Figure 1d and Figure 6). As the sliding time increases from 0 to 250 ps, the sp-C transforms to both the $sp^3$-C and $sp^2$-C hybridized states. Previous studies[7,24] reported that this self-passivation behavior of carbon structure mainly attributes to the repulsive force of H atom in base oil, but it is also contributed by the applied normal load and the bonding between graphene and a-C surface (Figure 3a). However, for the moderately or highly hydrogenated systems (18.8H/L/34.1H), the $sp^3$-C also tends to be transformed to the $sp^2$-C structure at the running-in period besides sp-C (Figure 6). This is related with the increased surface H content, weakening the effect of H in base oil on the a-C:H surface. Combined with the shearing effect, it promotes the $sp^3$-C structure evolved to the thermodynamically favorable $sp^2$-C structure.[35,36]

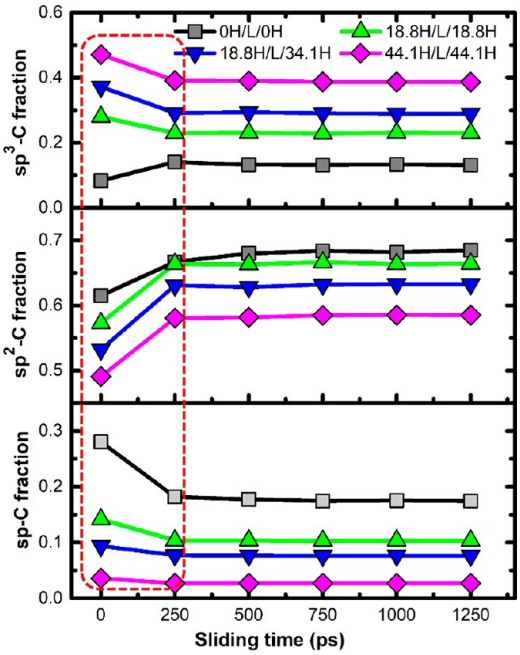


**Figure 6.** Evolution of the hybridized structure of friction interface ($sp^3$-C, $sp^2$-C, and sp-C) with sliding time for the systems of 0H/L/0H, 18.8H/L/18.8H, 18.8H/L/34.1H, and 44.1H/L/44.1H, respectively.

Previous studies[7−9] reported that under dry condition, due to the repulsive interaction between H atoms from mated a-C:H surfaces and H-induced interfacial passivation, hydrogenating the a-C surface promoted the easy shearing of friction interface, leading to the monotonous enhancement of antifriction capacity with H content of mated a-C:H surfaces. However, it is different from that under fluid lubricant condition. Figure 7a gives the stress distribution of H atoms in mated a-C:H surfaces during the sliding process. Figure 7b illustrates the hybridized structure of friction interface as a function of H contents of mated a-C:H surfaces. It can be seen that with increasing the surface H contents, the total stress values of H atoms in two a-C:H surfaces and $sp^3$-C fraction increase obviously, which is followed by the reduction of both the $sp^2$-C and sp-C fractions. But being different from the reports under dry condition,[8,9] the change of


https://doi.org/10.1021/acsami.1c09432
ACS Appl. Mater. Interfaces 2021, 13, 35173−35186

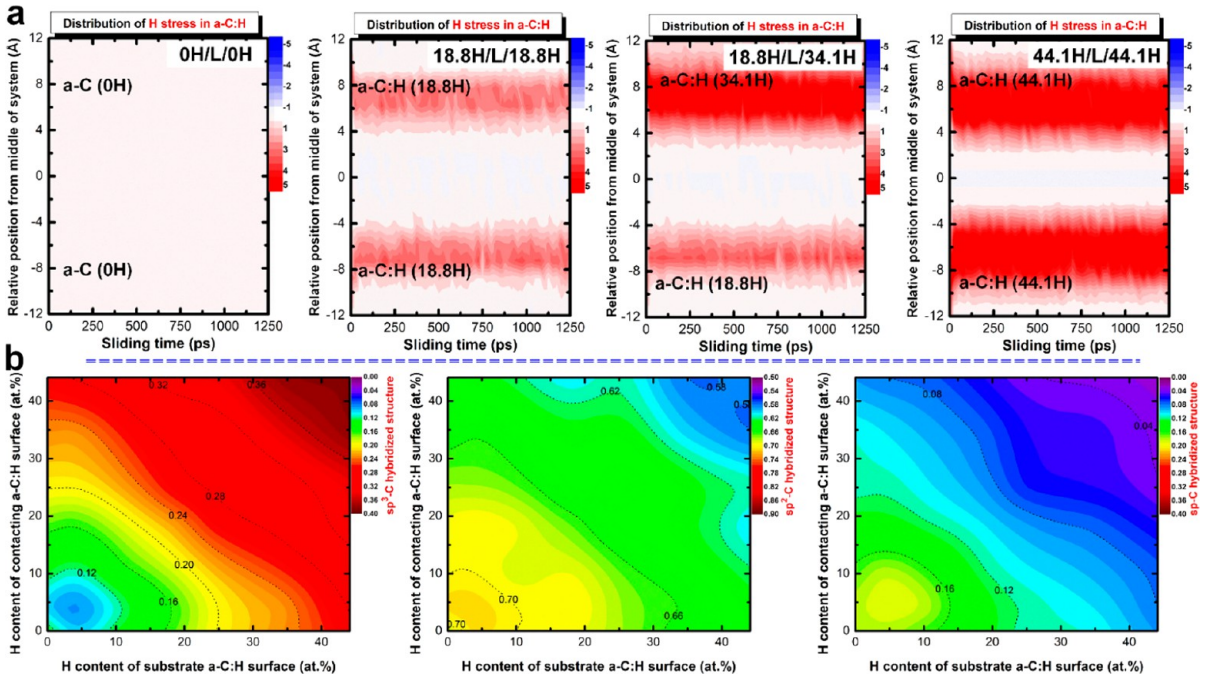


**Figure 7.** Stress distribution of H and hybridized structure of friction interface. (a) Stress distribution of H atoms in mated a-C:H surfaces during the sliding process (unit: GPa). (b) Dependence of interfacial hybridized structure on H contents of mated a-C:H surfaces after sliding time of 1250 ps, in which only the contributions from graphene and a-C:H are considered.

friction coefficient in Figure 2 is not exactly matched with the passivated degrees and H stress value of mated a-C:H surfaces. Especially, under the highly hydrogenated system, such as 44.1H/L/44.1H system, it has the lowest fraction of dangling bond and the highest value of H-induced repulsive stress while accompanied by the highest friction coefficient.

Moreover, Figure 8 gives the relationship between friction coefficient and sp-C hybridized structure of friction interface

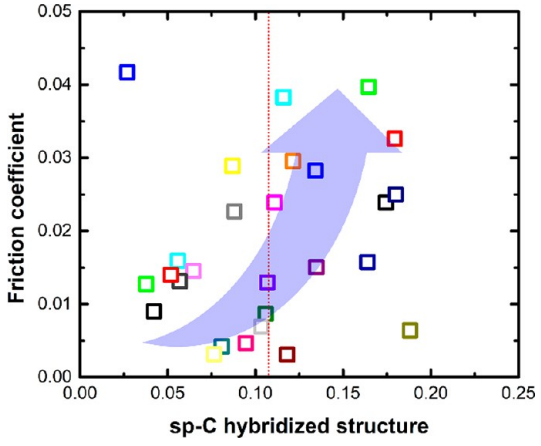


**Figure 8.** Relationship between friction coefficient and sp-C hybridized structure of friction interface after friction process.

after the sliding process. It reveals that for most of the cases, improving the hydrogenated degrees of mated a-C:H surfaces could reduce the dangling bonds at the sliding interface, which is favorable to the drop of friction coefficient. However, some systems, such as these marked with red dot lines in Figure 8, have a similar fraction of sp-C structure but a large difference in friction coefficient. This indicates that the H-induced passivation of friction interface may make the main contribution to the reduction of the friction coefficient. However, it must be also simultaneously influenced by other factors, such as the mobility of base oil molecules. Because the high repulsive value of H atoms in mated a-C:H surfaces (Figure 7a) may seriously suppress the mobility of base oil molecules, aggravate the intermolecular interaction between oil molecules, and thus increase the sliding resistance. This is different from the experimental and simulation results without fluid lubricant.[5−9]

**Diffusion Behavior of Base Oil Molecules at Friction Interface.** In order to evaluate the effect of hydrodynamic lubrication of base oil on friction behavior of nanocomposite system, the analysis of MSD curve is required.[24] Figure 9a first shows the results of base oil molecules for 0H/L/0H, 18.8H/L/18.8H, 18.8H/L/34.1H, and 44.1H/L/44.1H systems, respectively. It can be seen that the MSD value increases gradually with sliding time, but it is strongly dependent on the H content of a-C:H surface. The MSD values marked with gray background in Figure 9a are fitted to obtain the diffusion coefficient of base oil molecules along the sliding direction for each case. Figure 9b shows the dependence of diffusion coefficient of base oil on the hydrogenated degrees of mated a-C:H films. Note that with increasing the H contents of mated a-C:H surfaces, the diffusion coefficient of base oil tends to be increased first and then decreased. For example, in the 44.1H/L/44.1H system, the diffusion coefficient of base oil is only 0.273 $Å^2$/ps, while it reaches to 0.326 in 0H/L/0H, 0.385 in 18.8H/L/18.8H, and 0.463 $Å^2$/ps in 18.8H/L/34.1H, respectively. This change is related with the H-induced passivation (Figure 7) of friction interface, reducing the sliding resistance of a-C:H to base oil (Figure 9c), as also confirmed by previous study,[31] But it is also closely dependent on the repulsive force value of H from mated a-C:H surfaces (Figure 7a).

For the H-free case (0H/L/0H), although the anchoring of graphene additive can smooth the a-C surface, there are still many dangling bonds existed at the mated a-C surfaces (Figure


https://doi.org/10.1021/acsami.1c09432
ACS Appl. Mater. Interfaces 2021, 13, 35173−35186

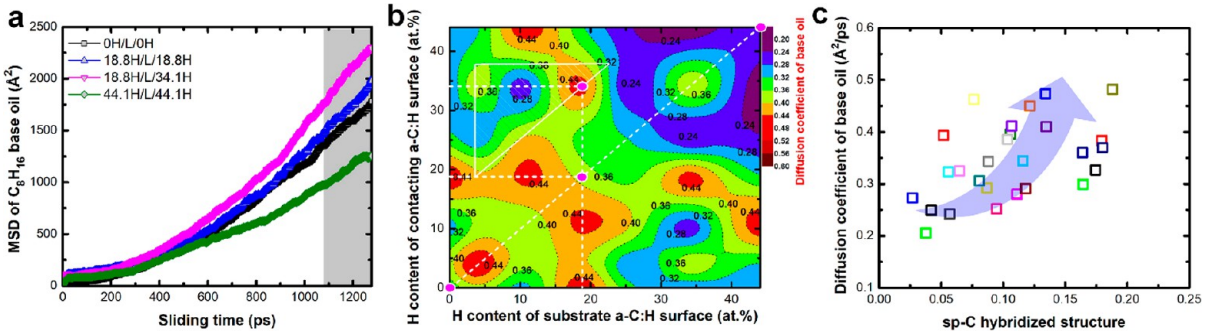


**Figure 9.** Diffusion behavior of base oil molecules at friction interface. (a) MSD curves of base oil molecules with sliding time for 0H/L/0H, 18.8H/L/18.8H, 18.8H/L/34.1H, and 44.1H/L/44.1H systems, respectively. (b) Dependence of diffusion coefficient of base oil on H contents of mated a-C:H surfaces (unit for diffusion coefficient: $Å^2$/ps). (c) Relationship between diffusion coefficient of base oil and sp-C hybridized structure of friction interface, in which only the contribution of C atoms from graphene and a-C:H to the hybridization is considered.

7b), resulting in the strong intermolecular interaction between base oil and two bare a-C surfaces. So the width of friction interface is only 18 Å; all base oil molecules, especially H atoms with repulsive stress in base oil, are localized to the small middle region of interface (marked with a dotted line in Figure 10a), limiting their mobility along the sliding direction. Following the increase of hydrogenated degree of a-C:H surface, such as in 18.8H/L/18.8H (Figure 10b) and 18.8H/L/34.1H (Figure 10c) systems, it reduces the fraction of sp-C dangling bonds (Figure 7b) at mated surfaces, weakening the intermolecular interaction of a-C:H surface to base oil. On the other hand, the H atoms in base oil tend to contact with two a-C:H surfaces. So the repulsive interaction between H atoms from a-C:H surfaces and base oil (Figures. 10b,c, and 7a) leads to the increase of interfacial width, improving the mobility of base oil molecules. As further increasing the H contents of mated a-C:H surfaces, such as 44.1H/L/44.1H in Figure 10d, the repulsive force value from H atoms of mated a-C:H surfaces (Figure 7a) is much higher than that of base oil molecules (Figure 10d). This high value causes the oil molecules close to each other and limited to the central region of friction interface, thus highly increasing the interaction between base oil molecules to prohibit their diffusion along the sliding direction.

In addition, with increasing the H contents of mated a-C:H surfaces, the presence of graphene additive also exhibits different effects on the diffusion of base oil. By comparison with the results without graphene additive in Figure 11, it can be seen that

- **Poorly hydrogenated a-C:H surface**, such as 0H/L/0H: the addition of graphene additive could significantly promote the mobility of base oil by chemical anchoring to smooth the active a-C surface.
- **Moderately hydrogenated a-C:H surface**, such as 18.8H/L/18.8H and 18.8H/L/34.1H systems: with further increasing the surface H contents of mated a-C:H surfaces, it results in the weak bonding or floating state of the graphene additive with a-C:H. The fluctuation of weak-bound graphene (Figure 5a) brings the inhomogeneous distribution of base oil (Figure 10) and additional resistance to the diffusion of base oil. However, it also contributes to the slight increase of interfacial width by its supporting role and thus loosens the distribution of base oil molecules to reduce their internal forces. This is confirmed by comparing with the system without graphene additive (SI Figure S4). So there is a slight increase of total MSD value of base oil in the system with additive as compared to that without graphene, as shown in Figure 11. In addition, the results also suggests that the oil diffusion in this condition is mainly up to the structures of mated a-C:H surfaces rather than additive.
- **Highly hydrogenated a-C:H surface**, such as 44.1H/L/44.1H: compared to the additive-free case, the addition of graphene additive decreases the MSD value of base oil, implying its negative effect. This is consistent with the result in Figure 5c. Although the graphene additive can also smooth the surface by physical adsorption (Figure 4d), it lows the repulsive force of a-C:H surface (SI Figure S3), accounting for the decreased mobility of base oil. The above-mentioned analysis reveals that with the increase of H contents of mated a-C:H surfaces, the contribution of graphene additive to the mobility of base oil changes from strengthening to weakening.

Furthermore, by further plotting the relationship of friction coefficient with H-induced interfacial passivation or mobility of whole base oil (Figure 8 and SI Figure S5), the friction behavior seems to be strongly dependent on the interfacial passivation rather than the mobility of fluid lubricant. This suggests the significant role of surface passivation, including chemical termination[40,41] or tribo-induced reconstruction,[15,42] in the improvement of friction behavior. However, the diffusion coefficient of base oil in Figure 9b represents the averaged mobility of the whole base oil molecules at the interface. Most importantly, Figure 10 (marked with dot lines) indicates that in the same system the hydrogenated degrees of mated a-C:H surfaces and the graphene additive could affect the distribution of base oil molecules at the friction interface, suggesting the coexistence of different diffusion behaviors.

In order to disclose this puzzle, the system located at the sliding time of 1125 ps is selected as reference configuration and the displacement of each atom in oil molecules along sliding direction during the following 125 ps is calculated, as illustrated in Figure 12. The displacement value is visualized by varying the particle color. For the substrate and contacting a-C:H films, the displacements are 0 and 12.5 Å, respectively, during 125 ps. However, the $C_8H_{16}$ oil molecules exhibit different displacement values and can be approximately divided into three parts: (i) the first one (named as $oil_{pf}$) is close to the top contacting a-C:H film, in which each atom has a positive displacement larger than 12.5 Å, suggesting the high mobility; (ii) the second one exhibits the negative value of displacement (<0), which contacts with the bottom substrate a-C:H surface, named as $oil_n$; (iii) the third one includes these with the displacement value between 0 and 12.5 Å (named as $oil_{ps}$) which can be distributed at the whole interface,


https://doi.org/10.1021/acsami.1c09432
ACS Appl. Mater. Interfaces 2021, 13, 35173−35186

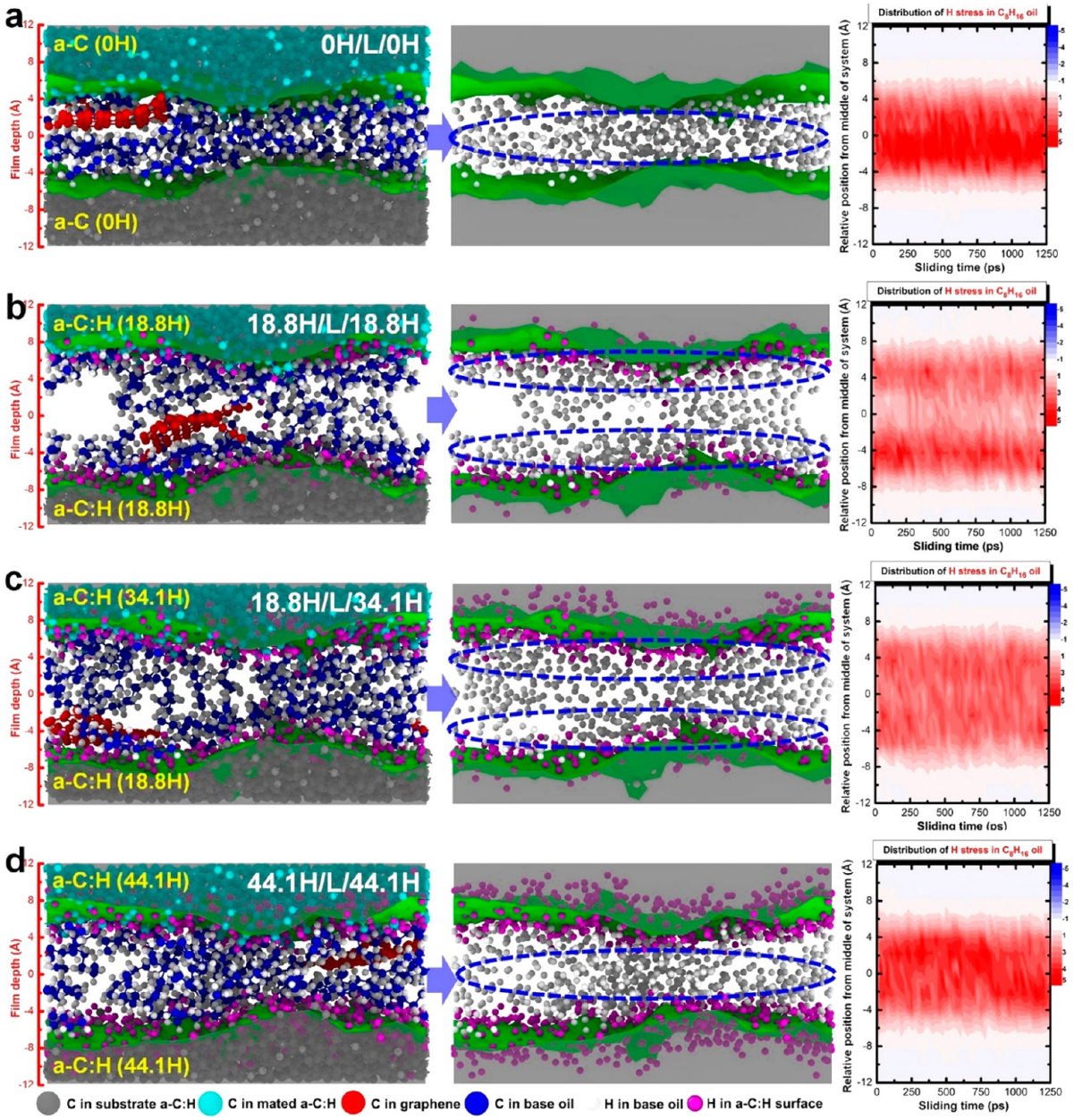


**Figure 10.** Morphologies and property of base oil molecules at the friction interface for (a) 0H/L/0H, (b) 18.8H/L/18.8H, (c) 18.8H/L/34.1H, and (d) 44.1H/L/44.1H systems, respectively, including the interfacial configurations, distribution of H atoms from a-C:H surfaces and base oil after sliding time of 1250 ps, and the stress distribution of H atoms in base oil with sliding time (unit for stress value: GPa).

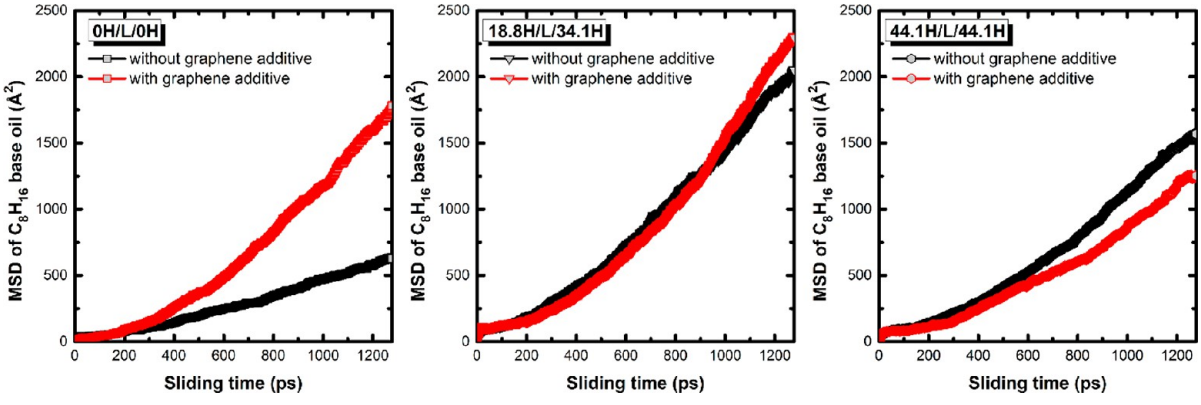


**Figure 11.** Comparison of MSD curves of $C_8H_{16}$ base oil in the systems with and without graphene additive, respectively.



https://doi.org/10.1021/acsami.1c09432
ACS Appl. Mater. Interfaces 2021, 13, 35173−35186

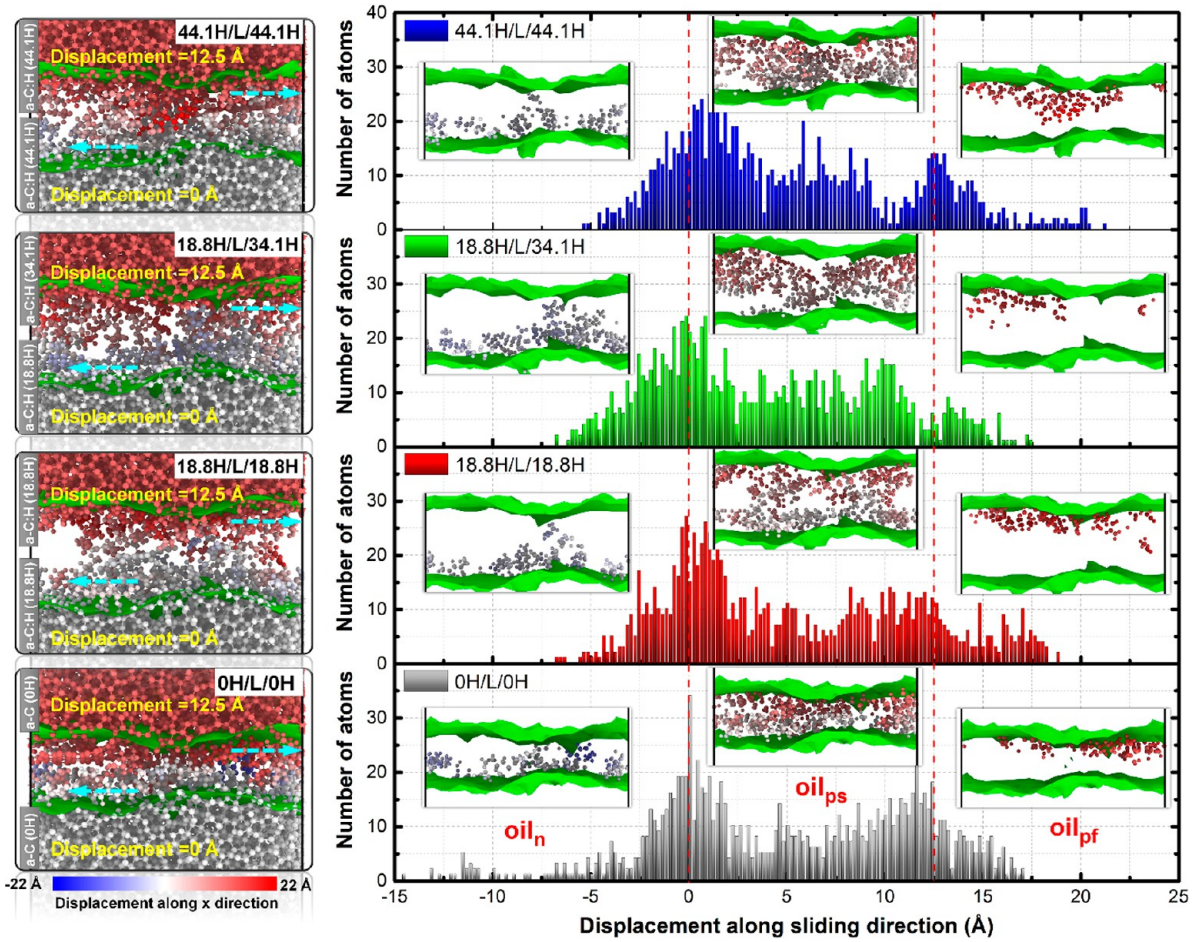


**Figure 12.** Displacement along *x* sliding direction of each atom in $C_8H_{16}$ molecules when the sliding time increases from 1125 to 1250 ps. The structure at the sliding time of 1125 ps is selected as a reference configuration.

but the displacement value of oil molecule tends to be dropped from top to bottom. This phenomenon has never been mentioned in any previous experimental and theoretical studies.

These complicated behaviors will not only cause the existence of additional force between these oil layers but also strong sensitivity to the mated a-C:H surfaces. For example, compared to the system with H-free (0H/L/0H) or highly hydrogenated (44.1H/L/44.1H) surface, in such system with moderate surface H content (18.8H/L/34.1H), these molecules in $oil_{ps}$ part are loosely distributed at the interface (Figure 12), reducing the internal sliding resistance. But most importantly, this unveils that the hydrogenation of a-C surface will cause the transformation of real sliding interface which dominates the friction resistance, and thus affect the friction behavior of synergy lubrication system, as will be discussed in the following part.

**Discussion on Friction Mechanism.** For the a-C:H/oil/graphene nanocomposite lubrication system, the above-mentioned analysis reveals that with increasing the hydrogenated degrees of mated a-C:H surfaces, it not only promotes the passivation of friction interface (Figure 7b), causing the binding state of graphene additive with a-C:H (Figure 5b) changed from anchoring to floating state, but also affects the mobility of base oil molecules via the H-induced repulsive effect (Figure 9b). Especially, the synergistic effect between base oil and a-C:H surface or graphene additive brings a significant difference in the distribution and diffusion behavior of base oil molecules at the friction interface (Figure 10 and Figure 12). This leads to the force simultaneously originated from six interactions, including contacting a-C:H/$oil_{pf}$, contacting a-C:H/$oil_{ps}$, $oil_{pf}$/$oil_{ps}$, $oil_{ps}$/$oil_n$, $oil_{ps}$/substrate a-C:H, and $oil_n$/substrate a-C:H, as illustrated in Figure 13a.

Being different from the case under dry condition,[9] in which the friction mainly occurs at the a-C:H/a-C:H interface, the introduction of fluid lubricant causes the real friction interface transformed to the a-C:H/oil composited interface and finally to the pure oil/oil interface as the oil content is enough.[43] Because $oil_{pf}$ and $oil_{ps}$ show different sliding directions with $oil_n$ and there is almost no contact between $oil_{pf}$ and $oil_n$ (Figure 12 and Figure 13a), the real friction response should occur at both the $oil_{ps}$/substrate a-C:H and $oil_{ps}$/$oil_n$ interfaces. The corresponding forces of $oil_n$ and substrate a-C:H to $oil_{ps}$ are named as $f_1$ and $f_2$, respectively. The signs of both the $f_1$ and $f_2$ are contrary to the sliding direction and thus resist the diffusion of base oil and the sliding of system. In addition, the internal resistance among $oil_{ps}$ molecules, $f_0$, should be also considered. So the friction force, $f$, can be approximately described as the following equation.

$$f = f_0 + f_1 + f_2 \tag{4}$$

These force values can be affected by the graphene additive, mobility of base oil, and H-induced repulsive stress and passivation of mated a-C:H surfaces.

Taking the systems of 0H/L/0H, 18.8H/L/18.8H, 18.8H/L/34.1H, and 44.1H/L/44.1H for examples, the effect of hydrogenating the a-C surface on the friction behavior of a-


https://doi.org/10.1021/acsami.1c09432
ACS Appl. Mater. Interfaces 2021, 13, 35173−35186

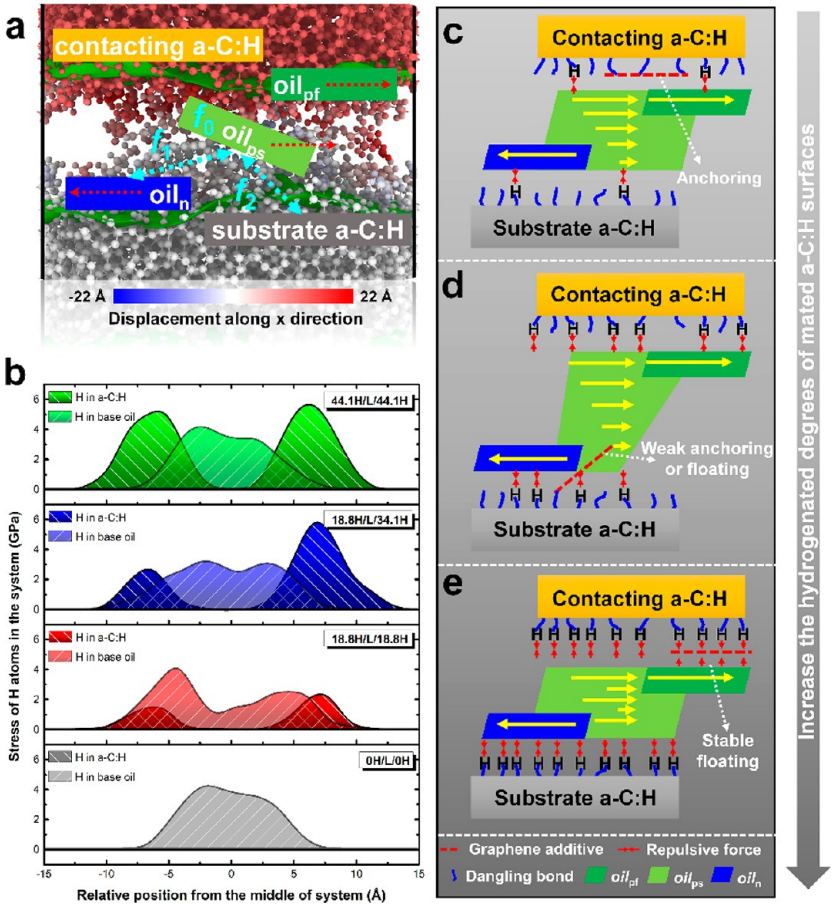


**Figure 13.** Discussion on friction mechanism. (a) Snapshots of friction interface at sliding time of 1250 ps as an example. (b) Stress distribution of H atoms from a-C:H surface and base oil molecules for each case at the sliding time of 1250 ps. (c), (d), and (e) are the corresponding schematic diagrams for underlying friction mechanisms of friction systems with bare or poorly, moderately, and highly hydrogenated a-C:H surfaces, respectively.

C:H/oil/graphene nanocomposite system and the underlying friction mechanism are discussed.

- **C:H/oil/graphene friction system with bare or poorly hydrogenated a-C:H, such as 0H/L/0H:** In this system, the graphene additive strongly anchors to the contacting a-C surface (Figure 3a). Compared to the additive-free case,[31] it can act as a protective film to smooth the sliding surface, shield partial intermolecular interaction of contacting a-C surface to enhance the mobility of base oil, thus contributing to the reduction of friction coefficient (Figure 2).[19,38,39] However, there are still many dangling bonds remained at the mated a-C:H surfaces (Figure 7b) following the strong intermolecular interaction to base oil. So these base oil molecules are uniformly adsorbed at each a-C surface to support the applied normal force, which are limited to the narrow interface (Figure 10a, Figure 12, Figure 13b, and SI Movie S1). This aggravates not only the internal shearing resistance of oil$_{ps}$ but also the interactions of oil$_{ps}$ with substrate a-C:H and oil$_n$, suggesting the high $f_1$, $f_2$, and $f_0$ values and thus explaining for the high friction coefficient (0.024) in Figure 2. The corresponding schematic diagram is demonstrated in Figure 13c.
- **C:H/oil/graphene friction system with moderately hydrogenated a-C:H, such as 18.8H/L/18.8H and 18.8H/L/34.1H:** it can be divided into two cases: one with self-mated a-C:H surface and the other composed of a-C:H surfaces with different H contents. For 18.8H/L/18.8H system, both the mated a-C:H surfaces are significantly passivated (Figure 7b). On the one hand, this weakens the intermolecular interaction of a-C:H surface to base oil molecules and thus decreases the value of $f_2$. On the other hand, this leads to the weak covalent bonding between graphene and a-C:H surface, as shown in Figure 3b and Figure 4b. The serious fluctuation of the unbonded part of graphene structure (Figure 5a) could prohibit the base oil against internal interaction, but it also plays a supporting role against the normal load. Combined with the repulsive interaction between H atoms from a-C:H surface and base oil (Figure 13b, Figure 7a, and Figure 10b), these result in the obvious increase of interfacial width and the loose distribution of oil molecules, reducing both the $f_0$ and $f_1$ values among oil$_{ps}$. However, as further increasing the H content of contacting a-C:H surface only, such as 18.8H/L/34.1H, there is obviously inhomogeneous distribution of oil$_{ps}$ molecules observed, which is different from that in the 18.8H/L/18.8H system (Figure 12). Especially, due to the passivation of contacting a-C:H surface, more molecules in oil$_{ps}$ show high mobility along the sliding direction, while fewer molecules interact with oil$_n$ and substrate a-C:H, thus further lowering the values of $f_1$ and $f_2$. Therefore, the superlow friction coefficient (Figure 2) is obtained. The corresponding schematic diagram for


https://doi.org/10.1021/acsami.1c09432
ACS Appl. Mater. Interfaces 2021, 13, 35173−35186

clarifying the antifriction mechanism is shown in Figure 13d.

- **C:H/oil/graphene friction system with highly hydrogenated a-C:H, such as 44.1H/L/44.1H:** as the mated a-C:H surfaces are highly hydrogenated, the graphene additive is stabilized at the a-C:H surface (Figure 4d) due to the repulsive effect of H atoms from a-C:H and base oil (Figure 13b, Figure 7a, and Figure 10d). However, this adsorption of graphene also weakens the high repulsive interaction of a-C:H surface (SI Figure S3), unfavorable to the mobility of base oil molecules and the reduction of friction coefficient, as confirmed by the result in Figure 5c. In particular, this extremely high repulsive force from both the a-C:H surfaces (Figure 13b) also causes the oil molecules localized at the middle of friction interface; the $oil_{ps}$ molecules with different sliding velocities mix seriously (Figure 12). This deteriorates the hydrodynamic lubrication property of base oil (Figure 9 and SI Movie S4) and increases the $f_0$, $f_1$, and $f_2$ values significantly (Figure 13e), although the a-C:H surface is highly passivated. Hence, the friction coefficient increases to 0.042 from 0.024 for the 0H/L/0H system (Figure 2).

As compared to that under dry condition, the system under lubricant condition unveils a similar friction mechanism, mainly depending on the passivation of friction interface and repulsive force of H atoms from a-C:H surface. However, the friction coefficient exhibits different dependence on the surface H content. This is due to the agglomeration of oil molecules squeezed by the high repulsive of H atoms from substrate/contacting a-C:H surfaces. To the best of our knowledge, there is no result reported in previous studies about this issue. Most importantly, according to the above-mentioned outcomes, we can also deduce the change of the relationship between friction behavior of system and surface H content with the working conditions, such as additive-free case, oil-starved or oil-rich conditions. For example, under the graphene-free condition, more H content is required to compensate the positive role of graphene, leading to the ultralow region deviated to the position with slightly higher H contents of mated a-C:H surfaces.

## 4. CONCLUSIONS

In this work, we have explored the friction behavior and its instability of a-C:H/oil/graphene nanocomposite lubrication system induced by surface hydrogenation at the atomic scale. With respect to the interaction between a-C:H surface and graphene, diffusion behavior of base oil, and transformation of interfacial structure, the underlying friction mechanism was discussed. Key conclusions are as following.

- With increasing the hydrogenated degrees of mated a-C:H surfaces, the friction coefficient tends to be decreased first and then increased. Especially, based on the optimized H contents of both the mated a-C:H surfaces, the superlow friction behavior (friction coefficient <0.003) can be achieved.
- Enhancing the hydrogenated degree of a-C:H surface promotes the passivation of friction interface. Combing with the repulsive force of H atoms from mated a-C:H surfaces, these can account for the instability of friction behavior.
- However, excessive hydrogenation results in the binding state of graphene additive with a-C:H surface changed from chemical anchoring to floating state, which is followed by the presence of negative effect on friction reduction. In addition, it also brings the squeezing effect to the distribution and diffusion behavior of oil molecules. Furthermore, the presence of different diffusion behaviors of oil molecules leads to the real sliding interface evolved from a-C:H/a-C:H interface under dry condition to a-C:H/oil and oil/oil composited interfaces. These phenomena have never been reported in previous experimental or simulation works.
- These findings not only disclose the effect of different hydrogenated degrees of a-C:H surface on the friction performance and the fundamental mechanism, but also suggest an effective method to develop the advanced solid−fluid lubrication system by tailoring the a-C:H structure.

## ■ ASSOCIATED CONTENT

### Supporting Information

The Supporting Information is available free of charge at https://pubs.acs.org/doi/10.1021/acsami.1c09432.

Distributions of density and coordination of fabricated a-C:H film along film depth direction after hydrogenation process (Figure S1). Interaction between mated a-C:H surfaces (Figure S2). Stress distribution of H atoms in a-C:H or $C_8H_{16}$base oil for 44.1H/L/44.1H system with or without graphene additive, respectively (Figure S3). Interfacial snapshots of 18.8H/L/18.8H and 18.8H/L/34.1H systems with and without graphene additive, respectively, at the sliding time of 1250 ps (Figure S4). Relationship between friction coefficient and diffusion coefficient of base oil (Figure S5) (PDF)

Movie S1: Sliding process of 0H/L/0H friction system (AVI)

Movie S2: Sliding process of 18.8H/L/18.8H friction system (AVI)

Movie S3: Sliding process of 18.8H/L/34.1H friction system (AVI)

Movie S4: Sliding process of 44.1H/L/44.1H friction system (AVI)

## ■ AUTHOR INFORMATION

### Corresponding Authors

**Xiaowei Li** − *School of Materials and Physics, China University of Mining and Technology, Xuzhou 221116, P.R. China; Key Laboratory of Marine Materials and Related Technologies, Zhejiang Key Laboratory of Marine Materials and Protective Technologies, Ningbo Institute of Materials Technology and Engineering, Chinese Academy of Sciences, Ningbo 315201, P.R. China*; orcid.org/0000-0002-7042-2546; Phone: 86-516-83591879; Email: lixw0826@gmail.com

**Aiying Wang** − *Key Laboratory of Marine Materials and Related Technologies, Zhejiang Key Laboratory of Marine Materials and Protective Technologies, Ningbo Institute of Materials Technology and Engineering, Chinese Academy of Sciences, Ningbo 315201, P.R. China*; orcid.org/0000-0003-2938-5437; Phone: 86-574-86685170; Email: aywang@nimte.ac.cn; Fax: 86-574-86685159

**Kwang-Ryeol Lee** − *Computational Science Center, Korea Institute of Science and Technology, Seoul 136-791, Republic of Korea*; Phone: 82-2-958-5494; Email: krlee@kist.re.kr; Fax: 82-2-958-5451

### Authors

**Xiaowei Xu** − *Key Laboratory of Marine Materials and Related Technologies, Zhejiang Key Laboratory of Marine Materials and Protective Technologies, Ningbo Institute of Materials Technology and Engineering, Chinese Academy of Sciences, Ningbo 315201, P.R. China*

**Jianwei Qi** − *School of Materials and Physics, China University of Mining and Technology, Xuzhou 221116, P.R. China*

**Dekun Zhang** − *School of Materials and Physics, China University of Mining and Technology, Xuzhou 221116, P.R. China*

Complete contact information is available at: https://pubs.acs.org/10.1021/acsami.1c09432


### Author Contributions

X.L., A.W., and K.R.L. designed the research. X.L. and X.X. performed the research. X.L., X.X., J.Q., and D.Z. analyzed data. X.L., X.X., A.W., and K.R.L. cowrote the paper. All authors contributed to the discussions and comments on the manuscript.

### Notes

The authors declare no competing financial interest.

## ■ ACKNOWLEDGMENTS

This work was supported by the National Science Found for Distinguished Young Scholars of China (52025014), National Natural Science Foundation of China (51772307), K.C.Wong Education Foundation (GJTD-2019-13), and the Nano Materials Research Program through the Ministry of Science and IT Technology (NRF-2016M3A7B4025402).

## ■ REFERENCES


(1) Robertson, J. Diamond-Like Amorphous Carbon. *Mater. Sci. Eng., R* **2002**, *37*, 129−281.

(2) Chen, X.; Li, J. Superlubricity of Carbon Nanostructures. *Carbon* **2020**, *158*, 1−23.

(3) Manimunda, P.; Al-Azizi, A.; Kim, S. H.; Chromik, R. R. Shear-Induced Structural Changes and Origin of Ultralow Friction of Hydrogenated Diamond-like Carbon (DLC) in Dry Environment. *ACS Appl. Mater. Interfaces* **2017**, *9*, 16704−16714.

(4) Cui, L.; Lu, Z.; Wang, L. Toward Low Friction in High Vacuum for Hydrogenated Diamondlike Carbon by Tailoring Sliding Interface. *ACS Appl. Mater. Interfaces* **2013**, *5*, 5889−5893.

(5) Dag, S.; Ciraci, S. Atomic Scale Study of Superlow Friction Between Hydrogenated Diamond Surfaces. *Phys. Rev. B: Condens. Matter Mater. Phys.* **2004**, *70*, 241401.

(6) Erdemir, A. The Role of Hydrogen in Tribological Properties of Diamond-Like Carbon Films. *Surf. Coat. Technol.* **2001**, *146−147*, 292−297.

(7) Bai, S.; Onodera, T.; Nagumo, R.; Miura, R.; Suzuki, A.; Tsuboi, H.; Hatakeyama, N.; Takaba, H.; Kubo, M.; Miyamoto, A. Friction Reduction Mechanism of Hydrogen- and Fluorine-Terminated Diamond-Like Carbon Films Investigated by Molecular Dynamics and Quantum Chemical Calculation. *J. Phys. Chem. C* **2012**, *116*, 12559−12565.

(8) Wang, Y.; Xu, J.; Ootani, Y.; Bai, S.; Higuchi, Y.; Ozawa, N.; Adachi, K.; Martin, J. M.; Kubo, M. Tight-Binding Quantum Chemical Molecular Dynamics Study on the Friction and Wear Processes of Diamond-Like Carbon Coatings: Effect of Tensile Stress. *ACS Appl. Mater. Interfaces* **2017**, *9*, 34396−34404.

(9) Li, X.; Wang, A.; Lee, K. R. Atomistic Understanding on Friction Behavior of Amorphous Carbon Films Induced by Surface Hydrogenated Modification. *Tribol. Int.* **2019**, *136*, 446−454.

(10) Li, H.; Xu, T.; Wang, C.; Chen, J.; Zhou, H.; Liu, H. Tribochemical Effects on the Friction and Wear Behaviors of a-C:H and a-C Films in Different Environment. *Tribol. Int.* **2007**, *40*, 132−138.

(11) Wang, L.; Cui, L.; Lu, Z.; Zhou, H. Understanding the Unusual Friction Behavior of Hydrogen-Free Diamond-Like Carbon Films in Oxygen Atmosphere by First-Principles Calculations. *Carbon* **2016**, *100*, 556−563.

(12) Alazizi, A.; Draskovics, A.; Ramirez, G.; Erdemir, A.; Kim, S. H. Tribochemistry of Carbon Films in Oxygen and Humid Environments: Oxidative Wear and Galvanic Corrosion. *Langmuir* **2016**, *32*, 1996−2004.

(13) Chen, X.; Yin, X.; Qi, W.; Zhang, C.; Choi, J.; Wu, S.; Wang, R.; Luo, J. Atomic-Scale Insights into the Interfacial Instability of Superlubricity in Hydrogenated Amorphous Carbon Films. *Sci. Adv.* **2020**, *6*, eaay1272.

(14) Kuwahara, T.; Romero, P. A.; Makowski, S.; Weihnacht, V.; Moras, G.; Moseler, M. Mechano-Chemical Decomposition of Organic Friction Modifiers with Multiple Reactive Centers Induces Superlubricity of ta-C. *Nat. Commun.* **2019**, *10*, 151.

(15) Li, X.; Wang, A.; Lee, K. R. Mechanism of Contact Pressure-Induced Friction at the Amorphous Carbon/Alpha Olefin Interface. *npj Comput. Mater.* **2018**, *4*, 53.

(16) Erdemir, A.; Ramirez, G.; Eryilmaz, O. L.; Narayanan, B.; Liao, Y.; Kamath, G.; Sankaranarayanan, S. K. R. S. Carbon-Based Tribofilms from Lubricating Oils. *Nature* **2016**, *536*, 67−71.

(17) Fan, X.; Xue, Q.; Wang, L. Carbon-Based Solid-Liquid Lubricating Coatings for Space Applications-A Review. *Friction* **2015**, *3*, 191−207.

(18) Zhang, L.; Pu, J.; Wang, L.; Xue, Q. Friction Dependence of Graphene and Carbon Nanotube in Diamond-Like Carbon/Ionic Liquids Hybrid Films in Vacuum. *Carbon* **2014**, *80*, 734−745.

(19) Li, X.; Zhang, D.; Xu, X.; Lee, K. R. Tailoring the Nanostructure of Graphene as an Oil-Based Additive: toward Synergistic Lubrication with an Amorphous Carbon Film. *ACS Appl. Mater. Interfaces* **2020**, *12*, 43320−43330.

(20) Bewilogua, K.; Hofmann, D. History of Diamond-Like Carbon Films-From First Experiments to Worldwide Applications. *Surf. Coat. Technol.* **2014**, *242*, 214−225.

(21) Wang, Y.; Su, Y.; Zhang, J.; Chen, Q.; Xu, J.; Bai, S.; Ootani, Y.; Ozawa, N.; Bouchet, M. I. D. B.; Martin, J. M.; Adachi, K.; Kubo, M. Reactive Molecular Dynamics Simulations of Wear and Tribochemical Reactions of Diamond like Carbon Interfaces with Nanoscale Asperities under $H_2$ Gas: Implications for Solid Lubricant Coatings. *ACS Appl. Nano Mater.* **2020**, *3*, 7297−7304.

(22) Liu, J.; Jiang, Y.; Grierson, D. S.; Sridharan, K.; Shao, Y.; Jacobs, T. D. B.; Falk, M. L.; Carpick, R. W.; Turner, K. T. Tribochemical Wear of Diamond-Like Carbon-Coated Atomic Force Microscope Tips. *ACS Appl. Mater. Interfaces* **2017**, *9*, 35341−35348.

(23) Mutyala, K. C.; Singh, H.; Evans, R. D.; Doll, G. L. Effect of Diamond-Like Carbon Coatings on Ball Bearing Performance in Normal, Oil-Starved, and Debris-Damaged Conditions. *Tribol. Trans.* **2016**, *59*, 1039−1047.

(24) Li, X.; Xu, X.; Zhou, Y.; Lee, K. R.; Wang, A. Insights into Friction Dependence of Carbon Nanoparticles as Oil-Based Lubricant Additive at Amorphous Carbon Interface. *Carbon* **2019**, *150*, 465−474.

(25) Ye, X.; Ma, L.; Yang, Z.; Wang, J.; Wang, H.; Yang, S. Covalent Functionalization of Fluorinated Graphene and Subsequent Application as Water-based Lubricant Additive. *ACS Appl. Mater. Interfaces* **2016**, *8*, 7483−7488.

(26) Lin, J.; Wang, L.; Chen, G. Modification of Graphene Platelets and Their Tribological Properties as A Lubricant Additive. *Tribol. Lett.* **2011**, *41*, 209−215.

(27) Xiao, H.; Liu, S. 2D Nanomaterials as Lubricant Additive: A Review. *Mater. Des.* **2017**, *135*, 319−332.

(28) Plimpton, S. Fast Parallel Algorithms for Short-Range Molecular Dynamics. *J. Comput. Phys.* **1995**, *117*, 1−19.

(29) Li, X.; Ke, P.; Zheng, H.; Wang, A. Structure Properties and Growth Evolution of Diamond-Like Carbon Films with Different Incident Energies: A Molecular Dynamics Study. *Appl. Surf. Sci.* **2013**, *273*, 670−675.

(30) Evans, D. J.; Holian, B. L. The Nose-Hoover Thermostat. *J. Chem. Phys.* **1985**, *83*, 4069−4074.
(31) Li, X.; Wang, A.; Lee, K. R. Tribo-Induced Structural Transformation and Lubricant Dissociation at Amorphous Carbon/Alpha Olefin Interface. *Adv. Theory Simul.* **2019**, *2*, 1800157.
(32) Berendsen, H. J. C.; Postma, J. P. M.; van Gunsteren, W. F.; DiNola, A.; Haak, J. R. Molecular Dynamics with Coupling to An External Bath. *J. Chem. Phys.* **1984**, *81*, 3684−3690.
(33) Wang, Y.; Yamada, N.; Xu, J.; Zhang, J.; Chen, Q.; Ootani, Y.; Higuchi, Y.; Ozawa, N.; Bouchet, M. I. D. B.; Martin, J. M.; Mori, S.; Adachi, K.; Kubo, M. Triboemission of Hydrocarbon Molecules from Diamond-Like Carbon Friction Interface Induced Atomic-Scale Wear. *Sci. Adv.* **2019**, *5*, eaax9301.
(34) Tavazza, F.; Senftle, T. P.; Zou, C.; Becker, C. A.; Van Duin, A. C. T. Molecular Dynamics Investigation of the Effects of Tip-Substrate Interactions during Nanoindentation. *J. Phys. Chem. C* **2015**, *119*, 13580−13589.
(35) Li, X.; Wang, Z.; Li, H.; Wang, A.; Lee, K. R. Fast Synthesis of Graphene with A Desired Structure via Ni-Catalyzed Transformation of Amorphous Carbon during Rapid Thermal Processing: Insights from Molecular Dynamics and Experimental Study. *J. Phys. Chem. C* **2019**, *123*, 27834−27842.
(36) Chen, S.; Xiong, W.; Zhou, Y.; Lu, Y.; Zeng, X. An Ab Initio Study of the Nickel-Catalyzed Transformation of Amorphous Carbon into Graphene in Rapid Thermal Processing. *Nanoscale* **2016**, *8*, 9746−9755.
(37) Hayashi, K.; Tezuka, K.; Ozawa, N.; Shimazaki, T.; Adachi, K.; Kubo, M. Tribochemical Reaction Dynamics Simulation of Hydrogen on A Diamond-Like Carbon Surface Based on Tight-Binding Quantum Chemical Molecular Dynamics. *J. Phys. Chem. C* **2011**, *115*, 22981−22986.
(38) Mao, J.; Zhao, J.; Wang, W.; He, Y.; Luo, J. Influence of the Micromorphology of Reduced Oxide Sheets on Lubrication Properties as A Lubrication Additive. *Tribol. Int.* **2018**, *119*, 614−621.
(39) Zhao, J.; Mao, J.; Li, Y.; He, Y.; Luo, J. Friction-Induced Nano-Structural Evolution of Graphene as A Lubrication Additive. *Appl. Surf. Sci.* **2018**, *434*, 21−27.
(40) Cui, L.; Lu, Z.; Wang, L. Probing the Low-Friction Mechanism of Diamond-Like Carbon by Varying of Sliding Velocity and Vacuum Pressure. *Carbon* **2014**, *66*, 259−266.
(41) Chen, X.; Zhang, C.; Kato, T.; Yang, X.; Wu, S.; Wang, R.; Nosaka, M.; Luo, J. Evolution of Tribo-Induced Interfacial Nanostructures Governing Superlubricity in a-C:H and a-C:H:Si Films. *Nat. Commun.* **2017**, *8*, 1675.
(42) Kuwahara, T.; Moras, G.; Moseler, M. Friction Regimes of Water-Lubricated Diamond (111): Role of Interfacial Ether Groups and Tribo-Induced Aromatic Surface Reconstructions. *Phys. Rev. Lett.* **2017**, *119*, No. 096101.
(43) Li, X.; Wang, A.; Lee, K. R. Role of Unsaturated Hydrocarbon Lubricant on the Friction Behavior of Amorphous Carbon Films from Reactive Molecular Dynamics Study. *Comput. Mater. Sci.* **2019**, *161*, 1−9.


https://doi.org/10.1021/acsami.1c09432
*ACS Appl. Mater. Interfaces* 2021, 13, 35173−35186